Hydrophobic mismatch of mobile transmembrane helices: merging theory and experiments. Biochim Biophys Acta

ARTICLE *in* BIOCHIMICA ET BIOPHYSICA ACTA · FEBRUARY 2012

Impact Factor: 4.66 · DOI: 10.1016/j.bbamem.2012.01.023 · Source: PubMed

4 AUTHORS, INCLUDING:

Santiago Esteban-Martín
Barcelona Supercomputing Center
31 PUBLICATIONS **623** CITATIONS

SEE PROFILE

Jesús Salgado
University of Valencia
95 PUBLICATIONS **1,755** CITATIONS

SEE PROFILE

Biochimica et Biophysica Acta 1818 (2012) 1242–1249

Contents lists available at SciVerse ScienceDirect

Biochimica et Biophysica Acta

journal homepage: www.elsevier.com/locate/bbamem

Hydrophobic mismatch of mobile transmembrane helices: Merging theory and experiments

Erik Strandberg [a], Santi Esteban-Martín [b], Anne S. Ulrich [a,c], Jesús Salgado [d,*]

[a] Institute of Biological Interfaces (IBG-2), Karlsruhe Institute of Technology (KIT), Karlsruhe, Germany
[b] Institute for Research in Biomedicine, Barcelona, Spain
[c] Institute of Organic Chemistry and Center for Functional Nanotechnology, KIT, Karlsruhe, Germany
[d] Institute of Molecular Science, University of Valencia, Paterna (Valencia), Spain

ARTICLE INFO

Article history:
Received 9 December 2011
Received in revised form 23 January 2012
Accepted 25 January 2012
Available online 2 February 2012

Keywords:
Orientation of transmembrane peptides
Dynamics of transmembrane peptides
Peptide tilt angle
Solid-state ^{2}H NMR
WALP peptide family
XWALP peptide family

ABSTRACT

Hydrophobic mismatch still represents a puzzle for transmembrane peptides, despite the apparent simplicity of this concept and its demonstrated validity in natural membranes. Using a wealth of available experimental ^{2}H NMR data, we provide here a comprehensive explanation of the orientation and dynamics of model peptides in lipid bilayers, which shows how they can adapt to membranes of different thickness. The orientational adjustment of transmembrane α-helices can be understood as the result of a competition between the thermodynamically unfavorable lipid repacking associated with peptide tilting and the optimization of peptide/membrane hydrophobic coupling. In the positive mismatch regime (long-peptide/thin-membrane) the helices adapt mainly via changing their tilt angle, as expected from simple geometrical predictions. However, the adaptation mechanism varies with the peptide sequence in the flanking regions, suggesting additional effects that modulate hydrophobic coupling. These originate from re-adjustments of the peptide hydrophobic length and they depend on the hydrophobicity of the flanking region, the strength of interfacial anchoring, the structural flexibility of anchoring side-chains and the presence of alternative anchoring residues.

1. Introduction

Biological membranes are highly dynamic assemblies of lipids and proteins in aqueous environments. The weak forces maintaining their integrity are similar as those involved in functional changes of proteins [1–4]; hence the mutual adaptation between membrane proteins and bilayer lipids has numerous physiological implications [5]. Well known examples related to membrane-thickness are the molecular sorting among cellular organelles [6,7], formation of lateral membrane domains [8] or the functional regulation of channels [4,9,10], receptors [11] and enzymes [12]. These phenomena are readily explained by the concept of hydrophobic matching/mismatch [13–18] whose physical basis has been rationalized by the "mattress" model [13,14]. The mismatch (Δd) is defined as the difference between the hydrophobic length of the protein (along its main molecular axis, d_p) and the equilibrium hydrophobic thickness of the lipid bilayer (d_b^0, see Fig. 1).

There can exist many different responses to mismatch [15]. From the lipid side, it may affect the overall bilayer thickness, with concomitant changes of phase properties, or it can promote lateral phase segregation [16,19]. On the protein part, the elastic energy of mismatch may favor oligomerization [20–22], lateral sorting and/or structural reorganizations [3,23]. Changes in the tilt angle (τ) of the complete molecule or of individual transmembrane (TM) segments are particularly effective for adjusting the projected (onto the membrane normal or *z*-axis) hydrophobic length of the protein (d_p^z, Fig. 1), and τ is thus a recurrently investigated parameter [4,10,15,23]. Which of the possible adaptation mechanisms predominates and how they occur at the molecular level are difficult questions, since the mismatch responses depend on the interplay of multiple weak forces which vary with the composition and physical properties of the membrane as well as the size, geometry, structure and dynamics of the protein. For example, in phase segregated membranes the lipid packing forces oppose peptide tilting [24]. Thus, although liquid-ordered domains are thicker than liquid-disordered domains, a higher lipid packing enthalpy in the first drives preferential sorting of *long* TM peptides into the second, despite concomitant larger tilts [24,25]. For big membrane proteins, however, whole-molecule tilting is energetically more costly [17] and the optimal hydrophobic coupling drives preferentially lateral sorting of lipid and protein molecules [6,7,26] and/or changes in the tilt of individual protein helices [4,9,10] accompanied by significant bilayer deformations [2,27,28].

Given the complexity of the hydrophobic mismatch phenomenon, its principles and consequences can be better understood from studies of simplified models [15]. However, investigations using single spanning TM peptides often give conflicting results [29]. Theory and

* Corresponding author at: Instituto de Ciencia Molecular, Universitat de València, C/Catedrático José Beltrán, Nº 2. 46980 Paterna (Valencia), Spain. Tel.: +34 963543016; fax: +34 963543273.
E-mail address: jesus.salgado@uv.es (J. Salgado).

0005-2736/$ – see front matter © 2012 Elsevier B.V. All rights reserved.
doi:10.1016/j.bbamem.2012.01.023

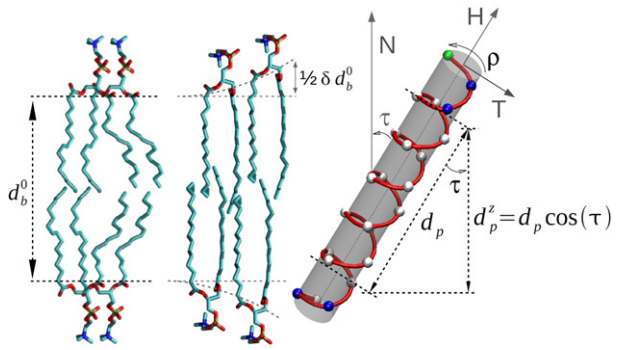

Fig. 1. Hydrophobic mismatch and orientation of transmembrane α-helical peptides. The peptide orientation is defined by the tilt angle (τ) between the helix axis (H) and the bilayer normal (N) and by the azimuthal rotation angle (ρ) around H. Usually, a stretch of hydrophobic residues in the peptide defines its standard hydrophobic length (d_p). This may be extended or reduced to an effective value (d_p^{eff}, not shown in the figure, but see the text) due to factors depending on the residues flanking the hydrophobic core. The mismatch (Δd) is the difference between d_p^{eff} and the intrinsic hydrophobic thickness of the lipid bilayer (free from distortion, d_b^0). Any adaptation between the membrane and the peptide occurs along the direction of the normal, where the projected peptide length (d_p^z) depends on the value of $cos(\tau)$. At positive Δd such a tilt response should be the dominant mechanism of adaptation, making $d_b^0 \approx d_p^z$. Each peptide residue is represented by a ball, colored green (first residue, used here to define ρ), blue (flanking residues as potential anchoring sites) or gray (hydrophobic residues).

molecular dynamics (MD) simulations predict that monomeric α-helical TM peptides adapt to positive mismatch (where the hydrophobic length of the peptide is larger than the hydrophobic thickness of the lipid bilayer) mainly and quantitatively by tilting, while producing only minor membrane thickening [1,17,18,30]. The small membrane distortion caused by TM peptides is supported experimentally [31–33]. Additionally, peptide tilting is favored thermodynamically against lateral sorting or oligomerization [24]. Clear responses of the tilt angle were obtained for various natural peptides and protein fragments, such as the TM helix of the M13 major coat protein (determined by fluorescence spectroscopy) [34], the pore-lining segment of influenza A virus M2 protein (by EPR) [35], and cell-signaling peptides containing nuclear localization sequences [36] and the channel-forming domain of Vpu from HIV-1 [37] (by PISEMA ^{15}N NMR). In contrast, the existing experimental results are confusing for model TM peptides of the WALP/WLP and KALP/KLP families (flanked by two W or two K, and with a core made of $-L(AL)_n-$ or $-L_n-$). From previous ^{2}H NMR studies, based on the *geometric analysis of labeled alanines* (GALA) method, these and other related peptides have displayed surprisingly small tilts which increase only very weakly upon decreasing membrane thickness [38–41]. This picture disagreed with results from MD simulations [18,42,43]. It was thus proposed that fast, large-amplitude fluctuations of the orientation angles of membrane peptides reduce the measured ^{2}H NMR splittings and lead to an underestimation of the tilt angles [44–47]. Although the simulation results have been contested [48], they are supported by independent ^{15}N NMR results on KALP-like peptides [49] and by recent investigations of WALP23 using fluorescence spectroscopy [50] and ^{2}H/^{13}C/^{15}N NMR [51]. Furthermore, this dispute has stimulated a revitalized interest in the influence of dynamics in studies of membrane-bound peptides by solid-state NMR [51–60]. To take orientational fluctuations into account, improved strategies have thus been developed for the analysis of ^{2}H NMR splittings, alone [52,56] or in combination with other anisotropic constraints [51].

Although there is today a growing consensus about the potential misinterpretation of experimentally determined orientations by NMR in highly dynamic systems [61], the orientational response of model TM peptides to hydrophobic mismatch awaits to be clarified. Here we address this problem through a comprehensive re-interpretation, using dynamical models [52], of complete sets of ^{2}H NMR splittings from published WALP/WLP [38–40], KALP/KLP [38] and XWALP [41,48] peptides in membranes of different thickness. The range of available data allows evaluating a wide range of mismatch conditions and provides a detailed description of mismatch-dependent effects on peptide orientation, which now compare favorably with theoretical predictions and MD simulations. For the examined cases we find that peptide tilting exerts a main contribution to hydrophobic mismatch adaptation. However, this effect is markedly dependent on the amino acid residues in the flanking sequence around the hydrophobic core, suggesting an essentially purely tilt-dependent adaptation for WALP/WLP and RWALP peptides, but deviating at large mismatch for KALP/KLP, WWALP, KWALP and GWALP peptides. The different behaviors can be understood by considering a competition between the thermodynamically costly peptide tilting and certain additional adaptations that change the effective hydrophobic length.

2. Theory and calculation

2.1. Interpretation of ^{2}H NMR data in a dynamical context

The orientation of α-helical peptides in membranes can be defined by the tilt angle τ, between the helix axis and the bilayer normal, and the azimuthal angle ρ, which describes the rotation around the helix axis usually with respect to the direction of the tilt (Fig. 1). Such information can be determined from experimental ^{2}H NMR quadrupolar splittings, measured on Ala-d_3 labeled peptides embedded in a lipid bilayer. The desired angles τ and ρ are obtained by fitting these data using the GALA model, which considers the structure of the peptide as a rigid canonical α-helix [39,40].

Advanced dynamical models for ^{2}H NMR data analysis are based on different ways of including the whole-body fluctuations of the peptide in the fitting procedure (*dyn*-GALA, details given elsewhere [52]). As we have reasoned previously, the most elaborate version of these *explicit* dynamical models utilizes Gaussian distributions for both τ and ρ to account for the fluctuating motions of the peptide around mean values of the two angles, which can be assumed to be fast on the NMR time scale [59]. The peptide dynamics are then described by the amplitude of these fluctuations, represented by the widths of the Gaussian distributions, σ_τ and σ_ρ, respectively. The effect of ρ fluctuations was shown to be the dominant parameter for transmembrane peptides [44,52]. For many of the systems studied here, only four Ala-d_3 labels were available in the literature and the sign of their splittings is unknown, so that only four absolute values can be used for fittings. Therefore, in order to avoid over-fitting in these cases, for the combined (comparative) analysis of different systems (Table 2 and Figs. 2 and 3) we fitted to three parameters only, namely τ, the mean of the ρ distribution (ρ_0), and the width of that distribution (σ_ρ), using $\Delta\nu^0_q = 74$ kHz.

The ^{2}H NMR data of WALP/WLP and KALP/KLP peptides had originally been analyzed in the literature using a quasi-static GALA model, where the only kind of dynamics considered was that present in dry peptide powder (corresponding to $\Delta\nu^0_q = 74$ kHz). Yet, the structure of the helix backbone had been made adjustable by including an additional free parameter, $\varepsilon_{||}$ (quasi-static fitted ε-model) [38–40]. This is the angle between the C_α–C_β bond and the helix long axis. In our analysis this angle was fixed at 58.9°, corresponding to a regular α-helix with torsion angles of $\varphi = -58°$ and $\psi = -47°$ [62]. The XWALP data were originally analyzed using a model including an adjustable molecular order parameter S_{mol}, keeping $\varepsilon_{||}$ fixed at 59.4° [41].

2.2. Error analysis

We used 90% confidence intervals of best-fit values to estimate the standard error of parameters. For that, the fits were performed at least 400 times with random errors added to each experimental quadrupole splitting. Such errors were random numbers produced

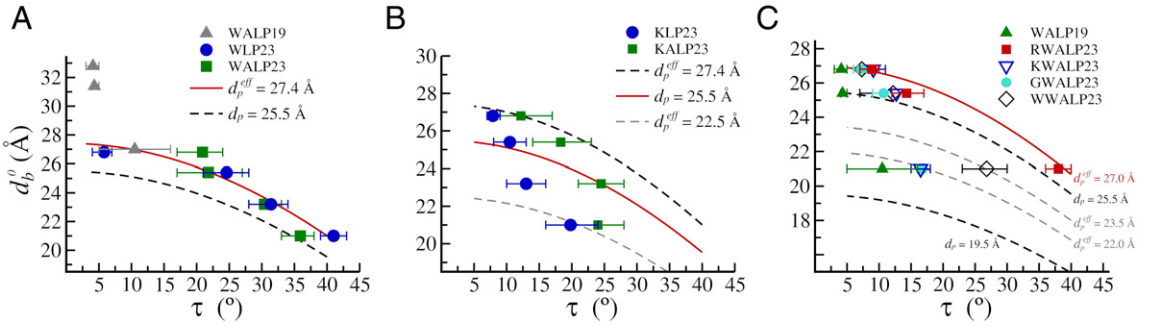

Fig. 2. Determining the effective peptide hydrophobic length. The projected peptide length, assumed equal to the known membrane thickness ($d_p^z \approx d_b^0$), is plotted against the measured peptide tilt angle τ for (A) WALP19, WALP23 and WLP23; (B) KALP23 and KLP23; (C) WALP19, RWALP23, KWALP23, GWALP23 and WWALP23. The τ angles were determined from *dyn*-GALA fits to experimental ^{2}H NMR quadrupolar splittings reported for these peptides in membranes of varying thickness (see Table 2) [38–41]. Fitting $d_b^0 \approx d_p^z = d_p^{eff}\cos(\tau)$ to these data points allows to find the corresponding values of d_p^{eff} (given for the respective curves in the panels). The values of $d_p = 25.5$ Å and $d_p = 19.5$ Å correspond to the expected lengths of the intrinsic hydrophobic cores (1.5 Å per residue) of 17 and 13 residues, respectively (dashed black curves). Values of d_p^{eff} selected for the mismatch analysis correspond to solid red curves; other values of d_p^{eff} correspond to gray dashed curves. In order to plot the points of WALP19 in panel (A), the values of the d_b^0 dimension were increased by $6\cos(\tau)$ Å, corresponding to 4 residues less compared to WALP23.

with the RAN1 function from Numerical Recipes in Fortran [63], with a uniform distribution in the range −1 kHz to +1 kHz around each particular data point. Data with added random errors were analyzed to get τ, ρ_0 and σ_ρ values. This way, the influence of experimental uncertainties was directly assessed for each peptide/lipid case studied, taking into account not only the uncertainty of the splitting but also the relative uncertainty and the number of data points. The number of runs was increased beyond 400 in some cases, but with negligible changes in the results. The best-fit parameters over all runs were represented by histograms and fitted to Gaussian distributions (see examples in Fig. S1), from which the mean and 90% confidence interval of each parameter were determined. In a few cases the histograms showed a superposition of two distributions, which were fitted independently and classified as *major* (area corresponding to >50% probability) and *minor* (area corresponding to <50% probability). In such bimodal cases of best-fit parameters, we used the values from the peak that included the "best fit" (made directly from the experimental splittings, with no random errors). This usually corresponded to the major distributions, except for WLP23 in DOPC and WWALP23 in DOPC. All used values extracted from the fitting procedures are listed in Table 2. For bimodal cases, values of the discarded distributions (in most cases the minor one) are listed in Table S1, in Supplementary Material. The plots represented in Figs. 2 and 3 were made with the values from Table 2, including 90% confidence intervals, which were used to determine the error bars.

2.3. Hydrophobic mismatch calculations

We define mismatch (Δ*d*) as the difference between the effective hydrophobic length of the peptide along its main helix axis (d_p^{eff}) and the equilibrium hydrophobic thickness of the lipid bilayer (d_b^0). For the determination of d_p^{eff}, please see Section 3 (and the values in Table 1). The hydrophobic thicknesses, d_b^0, of lipid bilayers used for this study are also listed in Table 1. These correspond to the length of acyl chains of lipids in the fluid phase, which for DLPC and DMPC bilayers have been obtained from X-ray diffraction data [64,65]. Because there are no measurements available for DTPC and DOPC bilayers, we calculated their thicknesses using the linear relationships deduced by Marsh [1,66], as follows: For a saturated acyl chain, with n_c denoting the number of aliphatic carbons, the length is given by:

$$d_b^0(n_c:0) = 2.21(n_c - 2.5)\ \text{Å} \quad (1)$$

and for a monounsaturated acyl chain the length is given by:

$$d_b^0(n_c:1) = 1.9(n_c - 3.9)\ \text{Å} \quad (2)$$

3. Results and discussion

3.1. Re-analysis of peptide orientation in a dynamical context

Peptides of the WALP and WLP series (WW-flanked, and terminated at the N- and C-termini with acetyl-G− and −A-amide, respectively, see Table 1) with lengths of 19 and 23 residues, and of the KALP and KLP series (KK-flanked) with a length of 23 residues, have been studied by ^{2}H NMR in membranes of DOPC, DMPC, DTPC and DLPC lipids [38–40]. A related family of recently developed peptides (XWALP23) was also analyzed [41,48]. These consist of a −L(AL)$_6$−

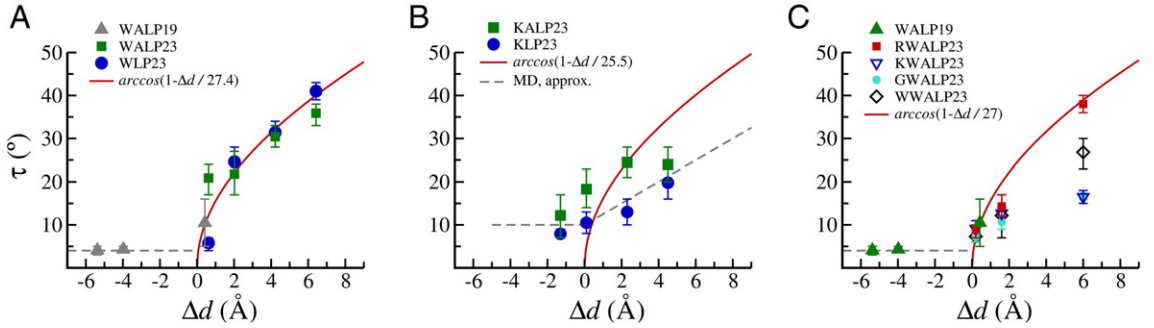

Fig. 3. Dependence of the peptide tilt angle, τ, plotted against the hydrophobic mismatch, Δ*d*, for (A) WW-flanked peptides, (B), KK-flanked peptides, and (C), and XALW-flanked peptides. At Δ*d*<0, the tilt appears constant at a minimum value (approximated by horizontal dashed lines). At Δ*d*>0 the solid red line represents the theoretical $\arccos(1-\Delta d/d_p^{eff})$ dependence that is expected for tilt-only adaptation. The gray dashed lines in panel (B) follow approximately the average behavior observed in an MD study [18].

Table 1
Length of peptides, thickness of membranes and corresponding hydrophobic mismatch for the peptide–lipid systems used in this work.

Peptide			Lipid, acyl chain composition (number of carbons:double bonds)/d_b^0 (Å)			
Name	Sequence[a]	d_p^{eff} (Å)[b]	DLPC 12:0/21[c]	DTPC 13:0/23.2[d]	DMPC 14:0/25.4[c]	DOPC 18:1/26.8[d]
KALP23	Ac-GKK–**L(AL)$_8$**–KKA-NH_2	25.5[e]	4.5	2.3	0.1	−1.3
KLP23	Ac-GKK–**L**$_{17}$–KKA-NH_2	25.5[e]	4.5	2.3	0.1	−1.3
WALP23	Ac-GWW–**L(AL)$_8$**–WWA-NH_2	27.4	6.4	4.2	2.0	0.6
WLP23	Ac-GWW–**L**$_{17}$–WWA-NH_2	27.4	6.4	4.2	2.0	0.6
WALP19	Ac-GWW–**L(AL)$_6$**–WWA-NH_2	21.4	0.4	–	−4.0	−5.4
WWALP23	Ac-GWALW–**L(AL)$_6$**–WLAWA-NH_2	27[e]	6.0	–	1.6	0.2
GWALP23	Ac-GGALW–**L(AL)$_6$**–WLAGA-NH_2	27[e]	6.0	–	1.6	0.2
KWALP23	Ac-GKALW–**L(AL)$_6$**–WLAKA-NH_2	27[e]	6.0	–	1.6	0.2
RWALP23	Ac-GRALW–**L(AL)$_6$**–WLARA-NH_2	27	6.0	–	1.6	0.2

[a] Residues of the hydrophobic core are highlighted in bold.
[b] Refined length after examination of the mismatch behavior (see text and Fig. 2), used to calculate the mismatch.
[c] Width of the acyl-chain region of the membrane determined from X-ray diffraction [64].
[d] Width of the acyl-chain region of the membrane determined from a linear dependence on the number of aliphatic carbons [1,66].
[e] Representative value for cases where d_p^{eff} is mismatch-dependent.

core, like in WALP19, but with only one W residue at each side which is flanked by the sequence acetyl-GXAL— at the N-terminus and by the sequence —LAXA-amide at the C-terminus (i.e. these XWALP23 peptides are XALW-flanked, with X being W, G, K or R). All peptide sequences are shown in Table 1. The investigated peptide/membrane combinations together cover a hydrophobic mismatch range between approximately −5.4 Å and +6.4 Å (see later). In order to re-evaluate the proper peptide orientations from the published raw data of these systems, we have developed an advanced version of GALA (*dyn*-GALA) [52]. This approach considers dynamical averaging of the ^{2}H quadrupolar splittings explicitly through Gaussian distributions of the orientation angles, i.e. the helix tilt τ and the azimuthal rotation ρ. Because in some cases the number of available quadrupole splittings is small (four values), the dynamical fits performed here include only distributions of ρ (see results in Table 2). We have shown previously that these fluctuations around ρ are the dominant dynamical averaging effect in monomeric TM helices [44,46,52]. We also notice that the present dynamical fits involve only three adjustable parameters {τ, ρ_0, σ_ρ}, i.e., the same number as in the previous studies that have used quasi-static models for data analysis.[1]

We found that the errors associated with the fits were always very low (root mean square deviation, rmsd ≤ 1.5 kHz, except for WALP23/DLPC and RWALP23/DLPC, see Table 2), often falling close to, or even below, the experimental error of ≈1 kHz. Thus, as a strategy for finding the most accurate solutions we calculated probability distributions of possible {τ, ρ_0, σ_ρ} parameters from the experimental data *via* Monte Carlo type calculations, from which we estimated 90% confidence intervals, as described in Section 2. The results are shown in Table 2. The tilt angles obtained in this way show, for each peptide, a clear dependence on the lipid chain length, as analyzed and discussed later.

3.2. Determination of peptide hydrophobic length

As introduced earlier, the hydrophobic mismatch is defined quantitatively as the difference Δ*d* between the hydrophobic length (d_p) of the peptide along its molecular axis and the hydrophobic thickness (d_b^0) of the bilayer (Fig. 1). Accurate values of d_b^0 can be obtained using linear relationships between the membrane thickness, from X-ray diffraction data [64,65], and the number of carbons in the lipid acyl chains, as reported by Marsh [1]. However, d_p is usually not measured experimentally and is most often taken as 1.5 Å (per residue rise in a perfect α-helix) multiplied by the number of residues in the hydrophobic core. This structural model assumes an ideal homogeneous conformation, at least within the hydrophobic core, which is generally supported by experiments [67]. A less justified, major approximation involved in this definition is the number of residues constituting the hydrophobic core. This number, in turn, depends on the identification of residues qualifying as *flanking*, i.e. those residues found to have a preference for the membrane interface region (usually the positively charged K or R, or the aromatic W or Y) where they can be expected to act as peptide anchors through specific polar interactions [68–71]. The model peptides considered here were designed specifically to contain at least one flanking residue at each end of the hydrophobic core (W or K, see sequences in Table 1). However, the simplest consideration of defining the innermost W or K as effective limits of the core may be an over-simplification. These residues exhibit hydrophobic character [72] (in the case of K due to the long aliphatic side chain [73]) and may interact favorably with the hydrocarbon part of the membrane. One should also take into account any hydrophobic contribution from residues further outside the inner flanking residues (for example, L^4 and L^{20} in XWALP23 peptides, see later), as well as the potential anchoring tendency of alternative *outer* flanking residues, which may force the inner flanks to become part of the core. Additionally, the hydrophobic length can be influenced by the local conformation of the anchoring side-chains, as well as distortions of the backbone structure around the anchoring positions. The latter may, for example, be important for peptides with a frayed helical conformation towards the termini, which is not unlikely [41].

Specifying all possible contributions to calculate the genuine hydrophobic length would need a detailed knowledge of peptide-membrane interactions and/or the structure of the peptide/membrane complex, which is typically not available. Instead, assuming that the projected peptide length d_p^z matches d_b^0, we analyzed the hydrophobic mismatch response for each peptide and evaluated its *effective* hydrophobic length, d_p^{eff}, from the experimentally accessible tilt angles τ. To this aim, we plotted for each series of different lipid chain lengths the known membrane thickness $d_b^0 \approx d_p^z$ against the corresponding changes in τ. The function $d_b^0 = d_p^{eff}cos(\tau)$ was fitted to these data points, since this angular (tilt) dependence is expected at positive mismatch, where the lipid response is found to be small in experiments and simulations [18,30,32], and the $d_p^z \approx d_b^0$ assumption is justified.

3.3. WW-flanked peptides (WALP and WLP) adapt to mismatch mostly by tilting

In the case of WALP23 and WLP23 (taken together, with $\tau > 5°$), a good fit to the $d_p^{eff}cos(\tau)$ curve is obtained for $d_p^{eff} = 27.4$ Å (Fig. 2A). This value is larger than the width of the thickest membranes used for the tilt measurements (DOPC with 26.8 Å) [38,39], which means

[1] In the previous analysis of ^{2}H NMR data [38–40], fits were made by considering a fixed molecular order parameter ($S_{zz} = 0.88$) and adjusting the two orientation angles of the peptide (τ and ρ) plus an internal structural angle ($^{\varepsilon}\|$), the latter accounting for possible deviations from the assumed canonical α-helical conformation.

Table 2
Peptide orientation and dynamical parameters from *dyn*-GALA fits, considering a fluctuating azimuthal rotation. Shown are results of best fits obtained directly from the analysis of measured splittings and from histograms of best fits corresponding to 400 runs with random errors in the splittings.

Peptide/lipid system	From measured splittings				From histograms of best fits using splittings with random errors[a]					
					Mean values			90% confidence intervals		
	τ (°)	ρ_0 (°)	σ_ρ (°)	rmsd (kHz)	τ (°)	ρ_0 (°)	σ_ρ (°)	τ (°)	ρ_0 (°)	σ_ρ (°)
KALP23/DLPC[b,g]	23	286	65	1.02	24.0	285.4	66.5	20–28	283-288	58-75
KALP23/DTPC[b,g]	24	286	78	0.18	24.5	285.3	78.8	21–28	282–288	71–87
KALP23/DMPC[b]	19	281	77	0.24	18.3	279.6	74.7	14–23	276–283	62–87
KALP23/DOPC[b]	12	273	79	0.70	12.2	272.1	79.0	7–17	267–278	56–102
KLP23/DLPC[b]	19	266	59	0.27	19.8	265.6	60.5	16–24	263–268	51–70
KLP23/DTPC[b]	13	264	45	0.35	13.0	264.3	44.3	10–16	261–267	27–62
KLP23/DMPC[b]	10	265	35	0.87	10.5	264.5	36.5	8–13	261–268	20–53
KLP23/DOPC[b]	8	264	37	1.29	7.9	264.2	32.2	7–9	260–268	15–49
WLP23/DLPC[b]	39	175	80	0.98	41.0	150.3[g]	85.1	39–43	148–153[g]	82–88
WLP23/DTPC[b,g]	31	180	85	0.15	31.4	179.4	85.8	28–34	177–182	81–90
WLP23/DMPC[b,g]	24	186	80	0.06	24.6	185.7	80.5	21–28	183–189	73–88
WLP23/DOPC[b,h]	5	180	28	0.92	5.8	175.7	24.3	4–7	169–182	12–37
WALP23/DLPC[c]	35	144	95	2.31	35.9	142.9	95.7	33–38	140–146	93–98
WALP23/DTPC[c]	30	145	96	1.45	30.4	144.9	96.1	28–33	142–148	92–100
WALP23/DMPC[c]	19	160	94	0.96	21.8	155.6	99.8	17–27	150–161	91–108
WALP23/DOPC[c]	21	153	113	0.52	20.9	152.0	112.8	17–24	147–157	104–122
WALP19/DLPC[d,g]	12	170	92	0.82	10.5	169.5	85.6	5–16	163–176	59–112
WALP19/DMPC[d]	4	195	24	0.93	4.3	194.4	24.4	4–5	190–199	9–40
WALP19/DOPC[d]	4	218	16	1.01	4.1	217.4	21.9[j]	3–5	212–222	7–37[j]
GWALP23/DLPC[e,g]	16	305	0	1.71	16.8	304.3	–[i]	16–17	302–306	0–13[i]
GWALP23/DMPC[e]	10	308	24	1.25	10.7	307.6	28.6	9–12	305–311	14–43
GWALP23/DOPC[e]	7	320	34	0.86	7.2	319.7	34.0	6–8	315–324	19–49
KWALP23/DLPC[e]	16	302	12	0.89	16.5	301.9	12.8	15–18	300–304	5–20
KWALP23/DMPC[e]	12	305	8	0.48	12.7	304.4	–[i]	12–14	302–307	0–32[i]
KWALP23/DOPC[e]	9	309	37	0.76	9.1	308.8	35.4	7–11	305–312	18–53
WWALP23/DLPC[e]	26	148	111	0.30	26.8	148.1	111.8	23–30	143–153	105–118
WWALP23/DMPC[e,g]	10	122	93	0.53	12.2	121.4	102.7	7–17	114–129	79–126
WWALP23/DOPC[e,h]	7	88	21	1.19	7.3	86.8	18.0	6–8	84–90	5–31
RWALP23/DLPC[e,g]	37	310	59	2.11	38.0	309.2	59.5	36–40	307–311	58–61
RWALP23/DMPC[e]	14	306	22	0.56	14.3	305.5	–[i]	12–17	303–308	0–45[i]
RWALP23/DOPC[e]	9	315	38	0.85	8.9	314.7	33.7	7–10	311–319	17–51
GWALP23/DLPC[f]	18	305	46	0.62	17.9	304.7	46.3	13–23	302–307	30–63

[a] The histograms were in turn fit to Gaussian distributions, of which we report the means and confidence intervals.
[b] Using ^{2}H NMR splittings from [38].
[c] Using ^{2}H NMR splittings from [40].
[d] Using ^{2}H NMR splittings from [39].
[e] Using ^{2}H NMR splittings from [41].
[f] Using ^{2}H NMR splittings from [48].
[g] The data correspond to the major (>50%) of two existing distributions, which in these cases contains the direct best-fit. The data from the minor distribution are in Table S1.
[h] The data correspond to the minor (<50%) of two existing distributions, which in these cases contains the direct best-fit. The data from the major distribution are in Table S1.
[i] Does not fit to a Gaussian. Confidence interval estimated from the complete histogram.
[j] Fit not including $\sigma_\rho = 0$.

that WALP23 and WLP23 were in all cases studied at positive mismatch. Additionally, it shows that the effective hydrophobic length of these two peptides is approximately 1.9 Å longer than expected when considering only the 17 hydrophobic residues as the core ($d_p = 25.5$ Å). This finding indicates that the inner flanking W residues, one at each end, are contributing to d_p^{eff}, and together amount to slightly more than one extra residue. This should not be surprising, given the pronounced hydrophobic character of W [70–72,74]. Furthermore, the hydrophobic contribution of the inner W residues may be enhanced here by a tendency of the two outer W residues to occupy anchoring positions. Other possibilities, like helix kinking and in general deviations from ideal helicity in the hydrophobic stretch, are considered unlikely. For example, a kink of a transmembrane helix would involve breaking hydrogen bonds between backbone groups which would be exposed to the hydrophobic interior of the membrane. Although this appears to be the case at least for the monomeric state of the M2 fragment of GABA(A) receptor, as suggested by MD simulations [22], the kink in this peptide is specifically stabilized *via* intramolecular hydrogen bonds with Ser and Thr side chains. A similar situation cannot occur for the core sequence of the model peptides studied here. In any case, such helix distortions should have direct consequences on the measured ^{2}H quadrupolar splittings (leading to a bad fit with the ideal helix model), which is not observed.

A view at conditions of negative mismatch for the WW-flanked peptides can be taken from the data points corresponding to WALP19 (Fig. 2A, gray triangles). This latter peptide has exactly the same sequence at the two ends as WALP23, but contains 4 residues less in its central core. Thus, to a good approximation, we can assume the length of WALP19 to be 6 Å shorter than for WALP23, giving a refined d_p^{eff} of 21.4 Å. Indeed, if we plot the data for WALP19 after correcting for its shorter core, i.e., by adding $cos(\tau) \times 6$ Å to the corresponding d_b^0, the tilt measured in DLPC follows nicely the same $d_p^{eff} cos(\tau)$ dependence as WALP23 (triangle at $d_b^0 \sim 27$ Å in Fig. 2A). The hydrophobic thickness of DMPC and DOPC membranes clearly surpasses the estimated hydrophobic length of WALP19 ($d_b^0 > 21.4$ Å, see Table 1), imposing negative mismatch, although yet τ remains at a minimum of ~4°. Non-zero minimum tilt angles at negative mismatch have been observed systematically in MD simulations [18] and can be attributed to the entropic contribution of helix precession about the membrane normal [75,76]. Nevertheless, it is clear that the strong negative mismatch cannot be alleviated through changes of tilt, and alternative mechanisms must operate. Likely possibilities are a local reduction of the membrane thickness near the peptide [31] and extra contributions of the flanking W residues to the hydrophobic length, i.e., an extra increase of d_p^{eff} (and d_p^z) at negative mismatch conditions. The latter can happen *via* deeper insertion

of the inner W residues while letting the outer W flanks occupy anchoring positions.

Using the values of d_b^0 and d_p^{eff} as determined earlier, we calculated the mismatch Δd for all WW-flanked peptides (Table 1) and plotted the peptide tilt angles against this parameter (Fig. 3A). This shows a clear representation of the different tilt responses and dependence on the mismatch regime. Thus, for WALP/WLP peptides, in all analyzed lipid systems, we conclude that tilting is sufficient to alleviate positive hydrophobic mismatch (Fig. 3A, solid line). i.e., the good agreement between the experimental and theoretical mismatch responses suggests that at least for these peptides additional contributions, like distortions of the peptide or the bilayer structures are negligible compared to the tilt only response. Notably, previous investigations of these peptides using the same ^{2}H NMR data had shown small and barely changing tilt angles with varying membrane thickness [38–40]. Comparing to those studies, the reason for the apparent divergence can be clearly attributed now to the importance of pronounced peptide orientational fluctuations, as suggested before [51,52,56], which had not been considered in the initial versions of the GALA data analysis. More recently, WALP23 has been also investigated using fluorescence spectroscopy and some large tilts with little mismatch response have been determined [50]. However, for the lipid membranes employed in that study one should expect near-matching or negative mismatch conditions, hence the invariable tilts are not surprising (although they are expected to be much smaller than reported).

3.4. The mismatch adaptation of KK-flanked peptides (KALP and KLP) involves a variable hydrophobic length

Except for DOPC membranes, KLP23 and KALP23 show systematically smaller tilt angles than their WW-flanked analogues (Table 2). Such differences are in good agreement with results of MD simulations [44] and must be attributed to the different polarity, anchoring properties, length and/or conformational freedom of K, compared to W. On the other hand, the tilts of KALP23 are larger than those of KLP23, although they are comparatively close to each other for the thickest and thinnest membranes. Therefore, the behavior of the KK-flanked peptides cannot be fit with the theoretical $d_b^0 \approx d_p^z = d_p^{eff} cos(\tau)$ function, unless we introduce a variable d_p^{eff}. At small positive mismatch (DOPC) the two KK-flanked peptides appear to exhibit a similar hydrophobic length as the corresponding WW-flanked peptides, ($d_p^{eff} = 27.4$ Å, Fig. 2B, black dashed curve). This suggests, as before, an elongation of the effective hydrophobic core by 1.9 Å. However, without such extension the bare hydrophobic core length ($d_p^{eff} = d_p = 25.5$ Å) gives the curve that passes through the tilt of KALP23 in DTPC and through the tilt of KLP23 in DMPC (Fig. 2B, red solid curve). Finally, the tilts of both peptides in the thinnest membranes (DLPC) seem to correspond to $d_p^{eff} \sim 22.5$ Å, suggesting an apparent reduction of the hydrophobic length (Fig. 2B, gray dashed curve). It thus appears that the KK-flanked peptides can re-adapt their effective hydrophobic length to a great extent to the actual membrane thickness, leading to a deviation of the peptide tilt from the behavior expected from theoretical considerations. To illustrate this, in Fig. 3B we have plotted the tilt angles of KALP23 and KLP23 using $d_p^{eff} = d_p = 25.5$ Å to calculate Δd. The observed elongation of the effective hydrophobic core in thicker membranes can be readily explained by the well known snorkeling of K [69,73,77]. The anchoring group in these residues is the charged $-NH_3^+$ at the tip of a long and flexible aliphatic side chain, whose position can be easily re-adjusted by conformational changes. The analysis further indicates that this extra contribution is reduced in thinner membranes, and for the shortest lipids (DLPC) apparently $d_p^{eff} < d_p$.

A mismatch dependent d_p^{eff} and an active role of K for hydrophobic peptide-membrane coupling via side chain snorkeling have been described with atomic detail by MD for KALP peptides, under a broad range of hydrophobic mismatch conditions [18]. Although the MD simulations may suffer from insufficient sampling, they show clearly that the flanking K residues help to alleviate negative mismatch by stretching their long aliphatic side chains from within the hydrophobic part of the membrane to keep their cationic amine groups at their preferred anchoring position near the phosphate oxygens of the phospholipids. This effect can increase the apparent hydrophobic length of the peptide by a few Å and keep the tilt angle for negative mismatch at a minimum value of ~10°, while concurrent with a local thinning deformation of the membrane [18]. At positive mismatch, the simulations predict an almost linear increase of τ. Our results for KLP23 (Fig. 3B, blue points) are in excellent agreement with the MD predictions (Fig. 3B, dashed line) throughout the complete set of analyzed data. The results from KALP23 at the two outermost mismatch points also agree with the MD simulations data, while the intermediate points deviate from linearity and approach the expected values for purely tilt-dependent adjustment (Fig. 3B, green points). All in all, these findings support the notion that the mismatch-dependent adaptation of KK-flanked peptides originates from a combination of multiple mechanisms, which differ depending on the mismatch regime. At positive mismatch the tilt-dependent adaptation dominates, but changes in the conformation of K side chains and local bilayer deformations may also exert important contributions. Apparently, the latter effects are thermodynamically more favorable than large peptide tilt angles, probably because peptide tilting involves a free energy cost for lipid re-packing [24,73].

3.5. Mismatch response of peptides with non-consecutive flanking residues (XWALPs)

An interesting case for the study of hydrophobic mismatch is the XWALP23 series of peptides [41,48] (which we denote here as XALW-flanked). As mentioned above, they share with WALP19 a 13 amino acids long hydrophobic core, flanked by inner W residues, but they also carry a second potential outer anchor at each end, separated by L and A from the inner W anchors (Table 1). We found that, in contrast to WALP19, XWALP23 peptides in DLPC show relatively large τ values which decrease steeply in DMPC and DOPC membranes (Table 2). Following the same reasoning as for WALP/WLP and KALP/KLP peptides, the apparent d_p^{eff} of all XWALP23 peptides in DOPC is ~27 Å (Fig. 2C, red curve). This corresponds to a considerable increase of the hydrophobic length, equivalent to ~5 residues with respect to the intrinsic 19.5 Å (the simplistic approximation for a core of 13 residues). Thus, in DOPC all four XWALP23 peptides seem to keep their putative inner flanking residues W^5 and W^{19}, plus at least L^4 and L^{20}, immersed within the acyl-chain region of the bilayer. Such a membrane binding state may be attributed to the pronounced hydrophobic character of L (in the case of GWALP23), and is probably also favored by the tendency of the outer flanking residues to occupy their preferred anchoring positions in the membrane interfacial region (in the case of KWALP23, WWALP23 and RWALP23).

The idea of a dominant anchoring contribution of the outermost flanking residues seems clear for the case of RWALP23, as the tilt of this peptide follows the theoretical dependence $\tau = arccos(1\text{-}\Delta d/27$ Å) at increased positive mismatch (at least up to Δd ~6 Å, Fig. 3C, squares). This behavior indicates that RWALP23 maintains a constantly elongated effective hydrophobic core, with interfacial anchoring through the R^2 and R^{22} residues and mismatch adaptation mainly *via* adjustments of the tilt. Such a tilt response of RWALP23 is comparable to that of WLP23 and WALP23 (Fig. 3A), for which we have above also proposed anchoring through the outer flanking residues (note also that RWALP23, WALP23 and WLP23 have their outer flanking residues at identical sequence positions, see Table 1). Thus, we conclude that these three peptides prefer to tilt, while anchoring *via* the outer flanking residues (and inserting L^4 and L^{20} in the case of RWALP23), despite the cost of large peptide tilts plus the cost of

displacing the inner flanking residues from an anchoring interfacial position.

In contrast, the tilt of WWALP23 (Fig. 3C, diamonds), and especially of GWALP23 and KWALP23 (Fig. 3C, circles and triangles-down), deviate from the initial curve as mismatch increases. These latter responses resemble those of KK-flanked peptides (Fig. 3B) and again indicate a decrease of the effective peptide hydrophobic length with increasing positive mismatch (Fig. 2C), although it does not reach the length corresponding to anchoring only *via* the inner W residues (d_p ~19.5 Å). Thus, for KWALP23 and WWALP23 increasing the peptide tilt angle appears to be more costly than weakening or losing the outer anchors, but still less costly than exposing L^4 and L^{20} to the hydrated interface, despite the anchoring tendency of inner flanking W residues. Since the thermodynamic cost of tilting, associated with perturbations of lipid packing enthalpy [24], should be similar for all peptides studied here (at least within the XWALP23 family) we may conclude that R is the "strongest" polar anchoring residue for phosphocholine lipids, followed by W and K, at least within the present peptide context. It is interesting to compare such an ordering of relative anchoring strength with calculated potentials of mean force (PMF), like that determined using umbrella sampling calculations on MD simulations [70] and the implicit potential derived by Ulmschneider et al. using statistical data [71]. The weakest anchoring of K can be predicted by the shallowest potential well of this residue in the membrane interface, compared to W and R [71]. On the other hand, although the PMF profiles in principle predict the strongest anchoring for W, the potential well of this residue is placed at a relatively deep position (near the peptide carbonyls) and extends into the hydrophobic region [70,71], while the well of R occupies a more external position, near the phosphate region. Thus, for the outermost W in WWALP23, it may by more difficult to reach an anchoring position in thin membranes than for R in RWALP23. Nevertheless, we should be cautious with these interpretations since other effects like possible fraying of the peptide termini may also play significant roles for the observed behavior of these peptides. Additionally, we may argue that the L^4 and L^{20} residues are effectively acting as hydrophobic anchors from within the acyl-chain region, which explains the very similar behavior of GWALP23 (without any outer flanking residues) and KWALP23. Such a *hydrophobic anchoring* effect of L appears to be stronger than the interfacial anchoring of inner W residues.

4. Concluding remarks

A careful analysis of ^{2}H NMR data from well known TM model peptides, considering explicit long-axial rotational fluctuations of the helices, provides a coherent view of hydrophobic mismatch effects on peptide orientation and dynamics. This comprehensive picture can explain earlier, seemingly contradictory results on the tilt response to mismatch, and illustrates new ways of adapting the effective peptide hydrophobic length through alternative anchoring residues.

For WW-flanked WALP23 and WLP23 in DMPC we find large tilt angles ($\tau = 22°–25°$) which in thinner membranes of DTPC and DLPC increase further to 30°–40°, indicating an extended hydrophobic length of these peptides compared to the intrinsic hydrophobic core. This effective extension appears to be favored by the tendency of the outer flanking W residues to bind at interfacial anchoring positions. The enhanced hydrophobic length is kept constant at increasing positive mismatch and the peptides follow the geometrical $d_b^0 = d_p^{eff} cos(\tau)$ rule, showing that tilting is the dominant adaptation effect.

In contrast, for KK-flanked peptides the effective hydrophobic length is markedly dependent on mismatch, which can be attributed to a variable contribution of snorkeling K side chains to hydrophobic coupling, possibly also accompanied by bilayer deformations. As a consequence, these peptides (especially KLP23) display a near-linear dependence of the tilt angle on mismatch, very similar to that predicted by MD simulations. It appears that changes in K side-chain conformations are energetically less costly than increasing the peptide tilt angle.

Finally, the new family of model peptides named XWALP23 allowed to compare the relative tendency of the outer pair (X) and inner pair (W) of flanking residues, separated by a helix turn containing a hydrophobic L residue. Here, the inner W and L residues contribute to a pronounced increase in the effective peptide hydrophobic length, compared to that expected by considering only the intrinsic hydrophobic core. The anchoring contribution of the outer pair of flanking residues is maintained at positive mismatch for RWALP23, which follows the theoretical $d_b^0 = d_p^{eff} cos(\tau)$ prediction in a way similar to WALP23 and WLP23. However, WWALP23, and especially KWALP23 and GWALP23, experience smaller tilt responses upon mismatch, suggesting that adaptation in these cases occurs *via* a reduction of the effective hydrophobic length d_p^{eff}.

Acknowledgments

This work was supported by the Spanish *MICINN* (BFU2010-19118/BMC, financed in part by the European Regional Development Fund), and by the DFG-Center for Functional Nanostructures in Karlsruhe (TP E1.2). SEM was supported by the European Molecular Biology Organization (Short Term fellowship). Dr. Stephan Grage is acknowledged for critical reading of the manuscript.

Appendix A. Supplementary data

Supplementary data to this article can be found online at doi:10.1016/j.bbamem.2012.01.023.

References

[1] D. Marsh, Energetics of hydrophobic matching in lipid–protein interactions, Biophys. J. 94 (2008) 3996–4013.
[2] O.S. Andersen, R.E. Koeppe, Bilayer thickness and membrane protein function: an energetic perspective, Annu. Rev. Biophys. Biomol. Struct. 36 (2007) 107–130.
[3] R. Phillips, T. Ursell, P. Wiggins, P. Sens, Emerging roles for lipids in shaping membrane-protein function, Nature 459 (2009) 379–385.
[4] O.P. Hamill, B. Martinac, Molecular basis of mechanotransduction in living cells, Physiol. Rev. 81 (2001) 685–740.
[5] A.G. Lee, How lipids affect the activities of integral membrane proteins, Biochim. Biophys. Acta 1666 (2004) 62–87.
[6] K. Mitra, I. Ubarretxena-Belandia, T. Taguchi, G. Warren, D.M. Engelman, Modulation of the bilayer thickness of exocytic pathway membranes by membrane proteins rather than cholesterol, Proc. Natl. Acad. Sci. U. S. A. 101 (2004) 4083–4088.
[7] H. Sprong, P. van der Sluijs, G. van Meer, How proteins move lipids and lipids move proteins, Nat. Rev. Mol. Cell Biol. 2 (2001) 504–513.
[8] J.A. Poveda, A.M. Fernández, J.A. Encinar, J.M. González-Ros, Protein-promoted membrane domains, Biochim. Biophys. Acta 1778 (2008) 1583–1590.
[9] M. Betanzos, C.-S. Chiang, H.R. Guy, S. Sukharev, A large iris-like expansion of a mechanosensitive channel protein induced by membrane tension, Nat. Struct. Biol. 9 (2002) 704–710.
[10] I.M. Williamson, S.J. Alvis, J. Malcolm East, A.G. Lee, Interactions of phospholipids with the potassium channel KcsA, Biophys. J. 83 (2002) 2026–2038.
[11] O. Soubias, S.-L. Niu, D.C. Mitchell, K. Gawrisc, Lipid-rhodopsin hydrophobic mismatch alters rhodopsin helical content, J. Am. Chem. Soc. 130 (2008) 12465–12471.
[12] C. Montecucco, G.A. Smith, F. Dabbeni-sala, A. Johannsson, Y.M. Galante, R. Bisson, Bilayer thickness and enzymatic activity in the mitochondrial cytochrome c oxidase and ATPase complex, FEBS Lett. 144 (1982) 145–148.
[13] O.G. Mouritsen, M. Bloom, Mattress model of lipid–protein interactions in membranes, Biophys. J. 46 (1984) 141–153.
[14] M. Sperotto, O. Mouritsen, Dependence of lipid-membrane phase-transition temperature on the mismatch of protein and lipid hydrophobic thickness, Eur. Biophys. J. 16 (1988) 1–10.
[15] J.A. Killian, T.K. Nyholm, Peptides in lipid bilayers: the power of simple models, Curr. Opin. Struct. Biol. 16 (2006) 473–479.
[16] M. Sperotto, J. Ipsen, O. Mouritsen, Theory of protein-induced lateral phase-separation in lipid-membranes, Cell Biophys. 14 (1989) 79–95.
[17] M. Venturoli, B. Smit, M.M. Sperotto, Simulation studies of protein-induced bilayer deformations, and lipid-induced protein tilting, on a mesoscopic model for lipid bilayers with embedded proteins, Biophys. J. 88 (2005) 1778–1798.
[18] S.K. Kandasamy, R.G. Larson, Molecular dynamics simulations of model transmembrane peptides in lipid bilayers: a systematic investigation of hydrophobic mismatch, Biophys. J. 90 (2006) 2326–2343.

[19] S. Morein, J.A. Killian, M.M. Sperotto, Characterization of the thermotropic behavior and lateral organization of lipid-peptide mixtures by a combined experimental and theoretical approach: Effects of hydrophobic mismatch and role of flanking residues, Biophys. J. 82 (2002) 1405–1417.
[20] A.V. Botelho, T. Huber, T.P. Sakmar, M.F. Brown, Curvature and hydrophobic forces drive oligomerization and modulate activity of rhodopsin in membranes, Biophys. J. 91 (2006) 4464–4477.
[21] I. Casuso, P. Sens, F. Rico, S. Scheuring, Experimental evidence for membrane-mediated protein-protein interaction, Biophys. J. 99 (2010) L47–L49.
[22] S.K. Kandasamy, D.-K. Lee, R.P.R. Nanga, J. Xu, J.S. Santos, R.G. Larson, et al., Solid-state NMR and molecular dynamics simulations reveal the oligomeric ion-channels of TM2-GABA(A) stabilized by intermolecular hydrogen bonding, Biochim. Biophys. Acta 1788 (2009) 686–695.
[23] T.K.M. Nyholm, S. Özdirekcan, J.A. Killian, How protein transmembrane segments sense the lipid environment, Biochemistry 46 (2007) 1457–1465.
[24] L.V. Schäfer, D.H. de Jong, A. Holt, A.J. Rzepiela, A.H. de Vries, B. Poolman, et al., Lipid packing drives the segregation of transmembrane helices into disordered lipid domains in model membranes, Proc. Natl. Acad. Sci. U. S. A. 108 (2011) 1343–1348.
[25] J. Domański, S.J. Marrink, L.V. Schäfer, Transmembrane helices can induce domain formation in crowded model membranes, Biochim. Biophys. Acta (2012), doi:10.1016/j.bbamem.2011.08.021.
[26] F. Dumas, M.C. Lebrun, J.-F. Tocanne, Is the protein/lipid hydrophobic matching principle relevant to membrane organization and functions? FEBS Lett. 458 (1999) 271–277.
[27] P.C. Jost, O.H. Griffith, R.A. Capaldi, G. Vanderkooi, Evidence for boundary lipid in membranes, Proc. Natl. Acad. Sci. U. S. A. 70 (1973) 480–484.
[28] J.F. Ellena, P. Lackowicz, H. Mongomery, D.S. Cafiso, Membrane thickness varies around the circumference of the transmembrane protein BtuB, Biophys. J. 100 (2011) 1280–1287.
[29] M.M. Sperotto, S. May, A. Baumgaertner, Modelling of proteins in membranes, Chem. Phys. Lipids 141 (2006) 2–29.
[30] T.M. Weiss, P.C. van der Wel, J.A. Killian, R.E. Koeppe II, H.W. Huang, Hydrophobic mismatch between helices and lipid bilayers, Biophys. J. 84 (2003) 379–385.
[31] M.R.R. de Planque, D.V. Greathouse, R.E. Koeppe II, H. Schafer, D. Marsh, J.A. Killian, Influence of lipid/peptide hydrophobic mismatch on the thickness of diacylphosphatidylcholine bilayers. A 2H NMR and ESR study using designed transmembrane alpha-helical peptides and gramicidin A, Biochemistry 37 (1998) 9333–9345.
[32] M.R.R. de Planque, J.A. Kruijtzer, R.M. Liskamp, D. Marsh, D.V. Greathouse, R.E. Koeppe II, et al., Different membrane anchoring positions of tryptophan and lysine in synthetic transmembrane alpha-helical peptides, J. Biol. Chem. 274 (1999) 20839–20846.
[33] S. Ramadurai, A. Holt, L.V. Schäfer, V.V. Krasnikov, D.T.S. Rijkers, S.J. Marrink, et al., Influence of hydrophobic mismatch and amino acid composition on the lateral diffusion of transmembrane peptides, Biophys. J. 99 (2010) 1447–1454.
[34] R.B. Koehorst, R.B. Spruijt, F.J. Vergeldt, M.A. Hemminga, Lipid bilayer topology of the transmembrane alpha-helix of M13 Major coat protein and bilayer polarity profile by site-directed fluorescence spectroscopy, Biophys. J. 87 (2004) 1445–1455.
[35] K.C. Duong-Ly, V. Nanda, W.F. Degrado, K.P. Howard, The conformation of the pore region of the M2 proton channel depends on lipid bilayer environment, Protein Sci. 14 (2005) 856–861.
[36] A. Ramamoorthy, S.K. Kandasamy, D.-K. Lee, S. Kidambi, R.G. Larson, Structure, topology, and tilt of cell-signaling peptides containing nuclear localization sequences in membrane bilayers determined by solid-state NMR and molecular dynamics simulation studies, Biochemistry 46 (2007) 965–975.
[37] S.H. Park, S.J. Opella, Tilt angle of a trans-membrane helix is determined by hydrophobic mismatch, J. Mol. Biol. 350 (2005) 310–318.
[38] S. Özdirekcan, D.T. Rijkers, R.M. Liskamp, J.A. Killian, Influence of flanking residues on tilt and rotation angles of transmembrane peptides in lipid bilayers. A solid-state 2H NMR study, Biochemistry 44 (2005) 1004–1012.
[39] P.C. van der Wel, E. Strandberg, J.A. Killian, R.E. Koeppe II, Geometry and intrinsic tilt of a tryptophan-anchored transmembrane alpha-helix determined by 2H NMR, Biophys. J. 83 (2002) 1479–1488.
[40] E. Strandberg, S. Özdirekcan, D.T. Rijkers, P.C. van der Wel, R.E. Koeppe II, R.M. Liskamp, et al., Tilt angles of transmembrane model peptides in oriented and non-oriented lipid bilayers as determined by 2H solid-state NMR, Biophys. J. 86 (2004) 3709–3721.
[41] V.V. Vostrikov, A.E. Daily, D.V. Greathouse, R.E. Koeppe, Charged or aromatic anchor residue dependence of transmembrane peptide tilt, J. Biol. Chem. 285 (2010) 31723–31730.
[42] W. Im, C.L. Brooks III, Interfacial folding and membrane insertion of designed peptides studied by molecular dynamics simulations, Proc. Natl. Acad. Sci. U. S. A. 102 (2005) 6771–6776.
[43] S. Esteban-Martín, J. Salgado, Self-assembling of peptide/membrane complexes by atomistic molecular dynamics simulations, Biophys. J. 92 (2007) 903–912.
[44] S. Esteban-Martín, J. Salgado, The dynamic orientation of membrane-bound peptides: bridging simulations and experiments, Biophys. J. 93 (2007) 4278–4288.
[45] S. Özdirekcan, C. Etchebest, J.A. Killian, P.F.J. Fuchs, On the orientation of a designed transmembrane peptide: toward the right tilt angle? J. Am. Chem. Soc. 129 (2007) 15174–15181.
[46] S. Esteban-Martín, D. Giménez, G. Fuertes, J. Salgado, Orientational landscapes of peptides in membranes: prediction of 2H NMR couplings in a dynamic context, Biochemistry 48 (2009) 11441–11448.
[47] L. Monticelli, D.P. Tieleman, P.F.J. Fuchs, Interpretation of 2H-NMR experiments on the orientation of the transmembrane helix WALP23 by computer simulations, Biophys. J. 99 (2010) 1455–1464.
[48] V.V. Vostrikov, C.V. Grant, A.E. Daily, S.J. Opella, R.E. Koeppe, Comparison of "Polarization inversion with spin exchange at magic angle" and "geometric analysis of labeled alanines" methods for transmembrane helix alignment, J. Am. Chem. Soc. 130 (2008) 12584–12585.
[49] U. Harzer, B. Bechinger, Alignment of lysine-anchored membrane peptides under conditions of hydrophobic mismatch: A CD, N-15 and P-31 solid-state NMR spectroscopy investigation, Biochemistry 39 (2000) 13106–13114.
[50] A. Holt, R.B.M. Koehorst, T. Rutters-Meijneke, M.H. Gelb, D.T.S. Rijkers, M.A. Hemminga, et al., Tilt and rotation angles of a transmembrane model peptide as studied by fluorescence spectroscopy, Biophys. J. 97 (2009) 2258–2266.
[51] A. Holt, L. Rougier, V. Réat, F. Jolibois, O. Saurel, J. Czaplicki, et al., Order parameters of a transmembrane helix in a fluid bilayer: case study of a WALP peptide, Biophys. J. 98 (2010) 1864–1872.
[52] E. Strandberg, S. Esteban-Martín, J. Salgado, A.S. Ulrich, Orientation and dynamics of peptides in membranes calculated from 2H-NMR data, Biophys. J. 96 (2009) 3223–3232.
[53] S. Esteban-Martín, E. Strandberg, G. Fuertes, A.S. Ulrich, J. Salgado, Influence of whole-body dynamics on 15 N PISEMA NMR spectra of membrane proteins: a theoretical analysis, Biophys. J. 96 (2009) 3233–3241.
[54] S. Esteban-Martín, E. Strandberg, J. Salgado, A.S. Ulrich, Solid state NMR analysis of peptides in membranes: influence of dynamics and labeling scheme, Biochim. Biophys. Acta 1798 (2010) 252–257.
[55] L. Shi, A. Cembran, J. Gao, G. Veglia, Tilt and azimuthal angles of a transmembrane peptide: a comparison between molecular dynamics calculations and solid-state NMR data of sarcolipin in lipid membranes, Biophys. J. 96 (2009) 3648–3662.
[56] T. Kim, S. Jo, W. Im, Solid-state NMR ensemble dynamics as a mediator between experiment and simulation, Biophys. J. 100 (2011) 2922–2928.
[57] K. Bertelsen, B. Paaske, L. Thøgersen, E. Tajkhorshid, B. Schiøtt, T. Skrydstrup, et al., Residue-specific information about the dynamics of antimicrobial peptides from 1H−15 N and 2H solid-state NMR spectroscopy, J. Am. Chem. Soc. 131 (2009) 18335–18342.
[58] V.V. Vostrikov, B.A. Hall, D.V. Greathouse, R.E. Koeppe, M.S.P. Sansom, Changes in transmembrane helix alignment by arginine residues revealed by solid-state NMR experiments and coarse-grained MD simulations, J. Am. Chem. Soc. 132 (2010) 5803–5811.
[59] C. Fares, J. Qian, J.H. Davis, Magic angle spinning and static oriented sample NMR studies of the relaxation in the rotating frame of membrane peptides, J. Chem. Phys. 122 (2005) 194908.
[60] S.K. Straus, W.R. Scott, A. Watts, Assessing the effects of time and spatial averaging in 15 N chemical shift/15 N-1H dipolar correlation solid state NMR experiments, J. Biomol. NMR 26 (2003) 283–295.
[61] A. Holt, J. Killian, Orientation and dynamics of transmembrane peptides: the power of simple models, Eur. Biophys. J. 39 (2010) 609–621.
[62] R.W. Glaser, C. Sachse, U.H.N. Dürr, P. Wadhwani, A.S. Ulrich, Orientation of the antimicrobial peptide PGLa in lipid membranes determined from 19 F-NMR dipolar couplings of 4-CF3-phenylglycine labels, J. Magn. Reson. 168 (2004) 153–163.
[63] W.H. Press, B.P. Flannery, S.A. Teukolsky, W.T. Vetterling, Numerical recipes in FORTRAN 77, The Art of Scientific Computing, 2nd ed, Cambridge University Press, 1993.
[64] N. Kucerka, Y. Liu, N. Chu, H.I. Petrache, S. Tristram-Nagle, J.F. Nagle, Structure of fully hydrated fluid phase DMPC and DLPC lipid bilayers using X-ray scattering from oriented multilamellar arrays and from unilamellar vesicles, Biophys. J. 88 (2005) 2626–2637.
[65] N. Kucerka, S. Tristram-Nagle, J.F. Nagle, Structure of fully hydrated fluid phase lipid bilayers with monounsaturated chains, J. Membr. Biol. 208 (2005) 193–202.
[66] D. Marsh, M. Jost, C. Peggion, C. Toniolo, Lipid chain-length dependence for incorporation of alamethicin in membranes: electron paramagnetic resonance studies on TOAC-spin labeled analogs, Biophys. J. 92 (2007) 4002–4011.
[67] R.C. Page, S. Kim, T.A. Cross, Transmembrane helix uniformity examined by spectral mapping of torsion angles, Structure 16 (2008) 787–797.
[68] I.T. Arkin, A.T. Brunger, Statistical analysis of predicted transmembrane α-helices, Biochim. Biophys. Acta 1429 (1998) 113–128.
[69] E. Granseth, G. Von Heijne, A. Elofsson, A study of the membrane–water interface region of membrane proteins, J. Mol. Biol. 346 (2005) 377–385.
[70] J.L. MacCallum, W.F.D. Bennett, D.P. Tieleman, Distribution of amino acids in a lipid bilayer from computer simulations, Biophys. J. 94 (2008) 3393–3404.
[71] M.B. Ulmschneider, M.S.P. Sansom, A. Di Nola, Properties of integral membrane protein structures: derivation of an implicit membrane potential, Proteins 59 (2005) 252–265.
[72] S.H. White, W.C. Wimley, Membrane protein folding and stability: physical principles, Annu. Rev. Biophys. Biomol. Struct. 28 (1999) 319–365.
[73] E. Strandberg, J.A. Killian, Snorkeling of lysine side chains in transmembrane helices: how easy can it get? FEBS Lett. 544 (2003) 69–73.
[74] J. Kyte, R.F. Doolittle, A simple method for displaying the hydropathic character of a protein, J. Mol. Biol. 157 (1982) 105–132.
[75] W. Im, J. Lee, T. Kim, H. Rui, Novel free energy calculations to explore mechanisms and energetics of membrane protein structure and function, J. Comput. Chem. 30 (2009) 1622–1633.
[76] J. Lee, W. Im, Transmembrane helix tilting: insights from calculating the potential of mean force, Phys. Rev. Lett. 100 (2008) 018103.
[77] J.A. Killian, G. von Heijne, How proteins adapt to a membrane-water interface, Trends Biochem. Sci. 25 (2000) 429–434.